Chemical Engineering Journal 111 (2005) 173–180

Chemical Engineering Journal

www.elsevier.com/locate/cej

Numerical prediction of outlet velocity patterns in solid–liquid separators

Michael J. Doby [a,*], Wanwilai Kraipech [b], Andrzej F. Nowakowski [a,c]

[a] *Chemical Engineering Department, UMIST, P.O. Box 88, Manchester M60 1QD, UK*
[b] *Department of Chemical Engineering, Srinakharinwirot University, Rangsit-Nakhonnayok Rd, Klong 16, Ongharak, Nakhonnayok 26120, Thailand*
[c] *Department of Mechanical Engineering, University of Sheffield, Mappin Street, Sheffield S1 3JD, UK*

Abstract

Three-dimensional simulations of incompressible fluid flow within hydrocyclone have been performed using the developed numerical technique. A discretization of the physical problem has been done by using a finite element method based on mixed approximation of the velocity and pressure space. The approach offers significant advantages in the solution process of convection dominated internal flows having one inlet and more than one outlet. It deals with the complex geometry of the head entry part of hydrocyclone. The boundary conditions represent forces and are efficiently incorporated into the numerical formulation. Such formulation is very useful since it allows modeling the characteristic velocity profile in the outlet. We investigate the interaction between the swirling flow and velocity profile at the outlet. The studies are carried out for fluids with different properties and can be extended to hydrocyclones with different geometrical configurations.

Keywords: Solid–liquid separators; Discharge angle; Hydrocyclone design; Numerical simulation

1. Introduction

The discharge of solid–liquid separators contains the information, which could possibly be used for better operational control. The work presented endeavors to establish a procedure for improving operation of hydrocyclones based on computational simulations. The complex nature of the flow in hydrocyclones drastically changes depending on the operating conditions. Since the hydrodynamics of a hydrocyclone are not clearly understood, the design and control of hydrocyclones are primarily based on empirical data. Due to the complicated nature of flow in a hydrocyclone, the models developed to predict the operation and control are still under development. Heiskanen [1] argued that hydrocyclone empirical models available for determining the operational state should be used carefully, because the models did not accurately control or predict the operation of a hydrocyclone. In spite of the shortcomings, the design process of hydrocyclones consists of using empirical models and classification curves, which are based on specific fluid properties. Plitt [2] proposed one of the first models, which used operational parameters and calculated the mean particle size to determine the operational state. Other empirical relationships have been proposed by Lynch and Rao [3] and Nageswararao et al. [4], which compare well with specific experimental data. In spite of the inaccuracies and uncertainties of the empirical models, steps have been made in improving the design of hydrocyclones as demonstrated by Chu and Luo [5]. Due to lack of complex empirical databases for different mixtures and geometries, various methods of controlling the operation of a hydrocyclone are considered.

In order to develop a good control technique, the significant variables to the operation must be determined. The primary operating parameter that can be controlled without changing fluid properties or measuring the solids in the under/overflow is the discharge angle from the apex. Assuming that two distinct operational states of hydrocyclone exist, which are the following: roping and spray. The states differ by the discharge profile from the apex. Roping tends to form a rope-like discharge, while spray resembles an umbrella. Concha et al. [6] points out that the best separa-

* Corresponding author.
E-mail address: m.doby@postgrad.umist.ac.uk (M.J. Doby).

1385-8947/$ – see front matter © 2005 Elsevier B.V. All rights reserved.
doi:10.1016/j.cej.2005.02.014

tion occurs near the formation of rope discharge. Similarly, Neesse et al. [7] states on a broader note that a hydrocyclone achieves the best separation at a transitional discharge phase between roping and spraying. Many researchers have tried to control the operation of a hydrocyclone by using varying non-obtrusive experimental techniques. Van Latum [8] suggested using X-ray imaging during operation to produce density profile cross-sections. Williams [9] used electrical impedance tomography, which produced a cross-section of an operating hydrocyclone. Petersen et al. [10] used image analysis as a controlling mechanism for the hydrocyclone, based on the discharge spray angle. Neesse et al. [11] developed a non-obtrusive manner of controlling the performance based on the angle of the spray discharge using a combination of techniques, which effectively controlled the operation of a hydrocyclone. Van Deventer et al. [12] demonstrated a method of calculating the angle of discharge with the inclusion of gravity. The method that was presented shows that the spray discharge proceeds through three distinct stages, which are the following: initial increasing of angle, flat and the gravitational driven regions [12]. With the calculation of the angle, determination of the operating performance of the hydrocyclone can be predicted as shown by Petersen et al. [10].

Deriving from the analysis of the discharge spray, we proposed a novel approach for controlling the operation of a hydrocyclone. The approach, which is an extension of the computational code of Nowakowski and Dyakowski [13] can be implemented in the design stage to effectively control the operation of the hydrocyclones, or can be applied as a tool to determine the effectiveness of an existing solid–liquid separator by calculating the discharge angle.

2. Problem formulation

In the study, the necessary numerical data are obtained using finite element approximation of incompressible viscous flow. The governing partial differential equations are the continuity equation and the Navier–Stokes equations. The former is a mathematical realization of the incompressibility of the flow, whereas the latter is momentum equation along with a linear constitutive law relating stresses to rates of strains. The primitive variable formulation is expressed in the most general and fundamental "stress-divergence" form [14]. The form is commonly used in finite element methods and rarely in finite difference or volume methods. The advantage of the "stress-divergence" form is that it permits formulation of physically meaningful Neumann boundary conditions via proper accounting of viscous forces.

2.1. Boundary conditions

Fig. 1 introduces the vertical cross-section of a hydrocyclone with the different parts of boundary conditions indicated.

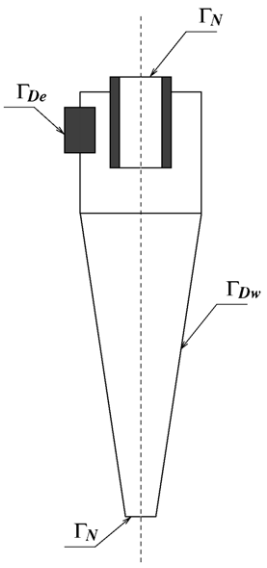

Fig. 1. Boundary conditions of hydrocyclone.

For fluid adjacent to a solid wall, Γ_{Dw} and at the inlet of the hydrocyclone, Γ_{De} the Dirichlet boundary conditions specifying the velocity vectors are imposed. At outflow sections, Γ_{N} Neumann boundary conditions are needed to truncate the computational domain. In the present application, they represent forces and are expressed by:

$$\boldsymbol{f} = \tau \boldsymbol{n} = -p\boldsymbol{n} + 2\nu \boldsymbol{D}(\boldsymbol{u})\boldsymbol{n} = \hat{\boldsymbol{f}} \tag{1}$$

where τ represents total stress tensor and $\boldsymbol{D}(\boldsymbol{u})$ deformation tensor equal to the following:

$$\tau = -p\boldsymbol{I} + 2\nu \boldsymbol{D}(\boldsymbol{u}) \qquad \boldsymbol{D}(\boldsymbol{u}) = 0.5[\nabla \boldsymbol{u} + (\nabla \boldsymbol{u})^{\mathrm{T}}] \tag{2}$$

here, $\boldsymbol{n}$ is unit outer vector normal to the boundary, $\hat{\boldsymbol{f}}$ the prescribed body force on the boundary, v denotes the kinematic viscosity of the fluid, $\boldsymbol{u}$ is the velocity vector and p is the scalar pressure. In the performed numerical simulations the "no-stress" boundary conditions were prescribed at the outlets. This is the equivalent of setting $\boldsymbol{f} = 0$ at the spigot and vortex finder outlet. Such assumption is physically correct, it does not pre-define the parameters of operations, although it may be considered idealistic. Clearly, the stresses exist and can play an important role in the establishment of the velocity profile. The precise value for such stresses is difficult to determine experimentally. Independent of mathematical legitimacy of such boundary conditions, the physics of the matter provides only guidance at best. However, with the lack of the necessary information, the assumption of zero-valued components of forces is natural and advantageous compared to the imposition of specific velocity profile as boundary conditions. The work of Nowakowski and Dyakowski [13] shows that such description has less significant impact on the velocity field. Consequently, the method proposed enables simulations of the characteristic velocity profile at the outlet. In contrast, majority of existing finite volume computational codes for hydrocyclones usually

specify the split ratio or make some assumptions regarding the character of the velocity profile. Such assumptions limit the applicability of simulations performed and consequently the obtained data cannot be used to control the operation of hydrocyclones. Another important advantage of boundary condition, Eq. (1), can be of use when modeling the air core (interface between fluids can be considered as a free boundary).

2.2. Numerical technique

In the finite element method, the flow equations and the associated boundary conditions are solved using the weak form of the governing equations. Then, the continuum problem governed by partial differential equations is reduced by discretization to a system of algebraic equations. The finite element procedure consists of meshing the hydrocyclone geometry into a number of tetrahedral elements. Within each of the elements, the dependent variables (three components of velocity and pressure) are interpolated by suitable polynomials at a set of nodal points. In the present implementation, the adopted element involves a piecewise continuous quadratic approximation of velocities and piecewise constant approximation of pressure. An account of the suitability of different approximation functions and element numerical stability for hydrocyclone simulation is presented in [15]. The comprehensive documentation of the finite element method applied to incompressible fluid mechanics was presented by Gresho and Sani [16].

2.3. Solution of flow problem

As a solution method, the pressure projection algorithm is implemented by Nowakowski and Dyakowski [13], which is based on some ideas introduced by Haroutunian et al. [17]. The method solves a convection–diffusion equation for velocity, excluding pressure from the momentum equations and updates the pressure while imposing the incompressibility constraint. The velocity field obtained in the first step does not satisfy continuity equation in general. Thus, the velocity field has to be projected onto a divergence-free subspace of the approximation space while updating the pressure. The above described procedure is carried out iteratively using the discrete operators after spatially discretizing the weak form of the Navier–Stokes equations. As a consequence, the boundary conditions, Eq. (1), are consistently incorporated in the algorithm.

2.4. Calculation of exit profile

The results of the computational fluid dynamics simulation of the hydrocyclone provide the data for calculating the discharge angle. Neesse et al. [7] showed that the form of the underflow discharge can be used as an indication of the operating state of hydrocyclones. The angle is determined from the velocity components at the spigot and fluid properties. Lacking the information from the three-dimensional flow field, Neesse et al. [7] derived the following equation:

$$\alpha = \arctan\left(\frac{v}{u}\right) \approx \arctan\frac{\rho_{\mathrm{m}}(D_u/2u)w^2}{\mu_{\mathrm{m}}} \tag{3}$$

here, u, v and w are the velocity components in the cylindrical coordinate system of the suspension in the axial (u), radial (v) and tangential direction (w), ρ_{m} the density of the mixture, μ_{m} the viscosity of the mixture and D_u is the apex diameter. Neesse et al. [7] model assumes boundary conditions that simplify the equations from a three- to two-dimensional problem. For simplification, the flow conditions at the inlet assume an axial symmetrical flow. The assumption of symmetrical flow is not an accurate representation of the flow in the hydrocyclone, as shown by He et al. [18]. The radial velocity was chosen by corresponding a flux to the given flow rate through the inlet. The model assumes that the viscosity of the fluid changes throughout the hydrocyclone, though in the present work the viscosity is set constant. The boundary conditions at the outlet assume that the effluent does not contact the air. Even with the simplifying assumptions for the method proposed by Neesse et al. [7], which will be referred to throughout the paper as the Dueck method, the Dueck method was able to be used to control the operation of the hydrocyclone.

The presented approach, which will be referred throughout the paper as the AFN method, is not limited to axisymmetrical flow. Thus, the AFN method having generated a three-dimensional velocity field the angle is calculated directly. Due to the three-dimensional nature of the problem, the complete set of Navier–Stokes equations was solved in a three-dimensional framework. The necessary velocity field profiles are obtained using the described finite element approach. An unstructured grid that forms to the shape of a hydrocyclone using tetrahedral elements is generated. One of the reasons that a structured grid was not used may be attributed to a singularity that occurs with the governing equations [19]. Using an unstructured grid helps not only to eliminate the occurrence of singularities but provides full geometrical flexibility. The computer output is in the form of velocity vectors in the u, v and w directions in a Cartesian coordinate system. Using basic trigonometric functions the calculation of the angle is obtained.

Table 1
Fluid properties at different runs with diameter at 22 mm

Number	Reynolds number (Re_{in})
Run 1	220
Run 2	259
Run 3	293
Run 4	338
Run 5	440
Run 6	488
Run 7	505

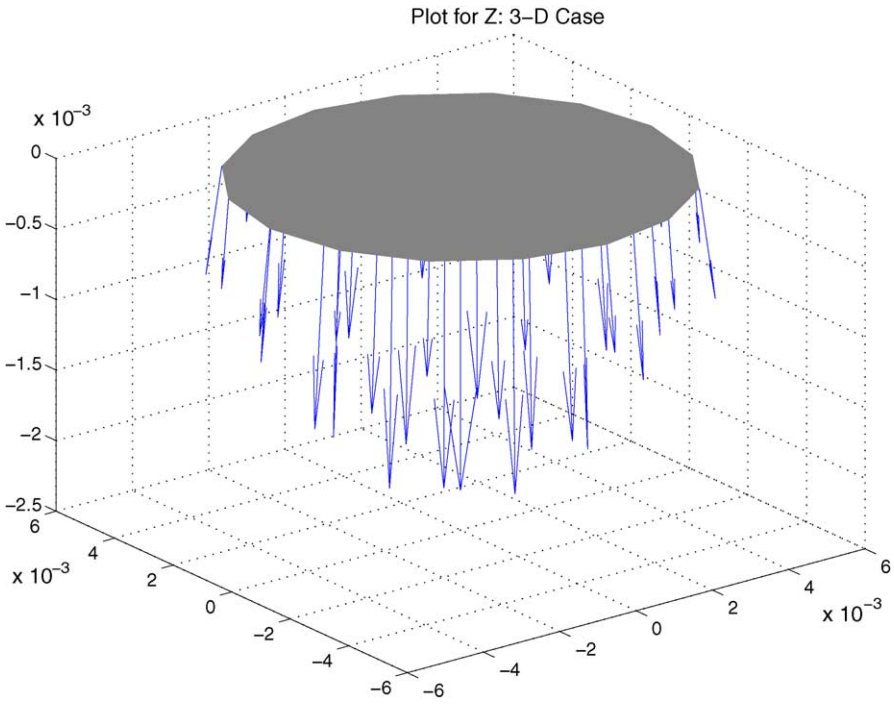

Fig. 2. Three-dimensional quiver cross-section of the velocity profile exiting the apex.

3. Results and discussion

In order to compare the results of the two methods, several formed at different Reynolds numbers at the inlet. The range of viscosities that were chosen kept the flow in the laminar regime. Due properties, the comparison would not introduce any questionable results from using a specific turbulence model. Laminar flow would be equivalent to feeding a viscous slurry in the hydrocyclone. For both methods, the angle calculations were performed for the same numerically obtained velocity data. In order for equal comparison, the viscosity in the computational domain was assumed to be constant for the Dueck method. Though the neglection of turbulence hydrocyclones is significant even with low inlet Reynolds numbers, a general behavior of the discharge angle can be seen to develop. Table 1 presents the numerical experiment by showing the changes in the Reynolds number at the inlet duct.

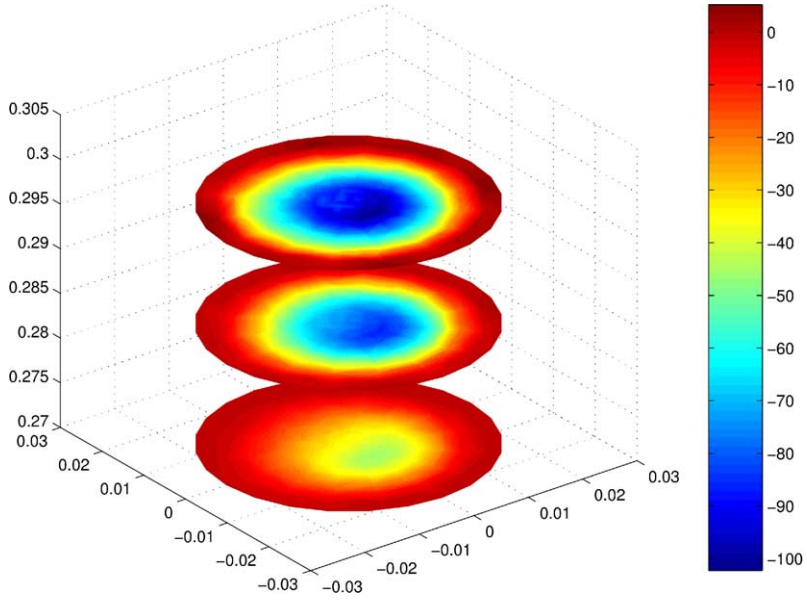

Fig. 3. Cross-section of the pressure profile at the height of 27, 28 and 29 cm.

The Reynolds number was calculated by $Re_{in} = \rho VD/\mu$, where ρ is the density, D the diameter and μ is the dynamic viscosity. The viscosities values decreased after the initial run to compare the change in the form of discharge. Due to the properties of the fluid, the hydrocyclone was operating in the roping region, as shown in Fig. 2.

For clarification, the solid-colored circular contour indicates the location of the exit. As can be seen from Fig. 2, the angle of the exiting fluid is predominately in the downward direction. The roping region can be distinguished from a spray discharge by observing the angle at which the slurry exits along the outer rim of the apex. The roping state tends to show that at the outer edge of the apex the discharge angle is closer to 90 than in spray discharge. However, operating in the experimented region, spray discharge does not occur.

Though in the model we did not take into account the air core, our model reveals the likely mechanism of air core creation. Atmospheric pressure at the center of the apex is the reference point for the pressure field in the hydrocyclone. As noticed in Fig. 3, a pressure reduction occurs toward the center of the hydrocyclone in each of the three different cross-sections. The lowest cross-section indicates that sediment has started to hinder the formation of the low pressure near the center.

As Fig. 3 shows, the bottom of the hydrocyclone has already been semi-plugged with sediment, thus not allowing the low-pressure field to develop at the tip. However, the examination of Fig. 4 reveals that the flow is moving away from the center at the apex.

Processing the data consists of using basic trigonometric functions and using Eq. (3) to calculate the discharge angle. The results of the angle calculated at different viscosities were compared between the AFN and Dueck methods and are listed in Table 2 below.

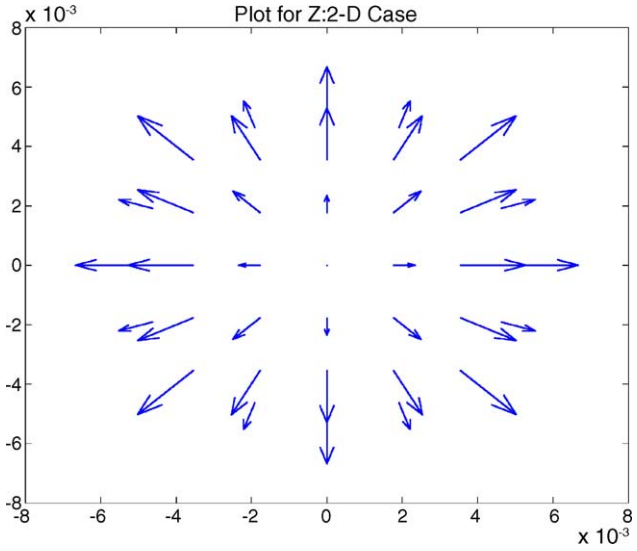

Fig. 4. The two-dimensional velocity profile projected onto the x–y plane cross-section at the apex.

The specific numerical data is not as important as the trend that is shown over the increasing viscosities. The comparison of the results obtained from both methods presents an interesting occurrence. The presented AFN method shows that the angle actually slightly decreases with increasing viscosity. The Dueck method predicts less of a change in the angle than the AFN method at corresponding outlet points. Since the operational state of the hydrocyclone is in roping, the expected angle exiting the spigot should be approximately 90°, which is predicted by both methods at constant viscosity. The possible cause of the inversion trend of the discharge angle at the apex in both methods could be due to the high pressure that occurs at the apex.

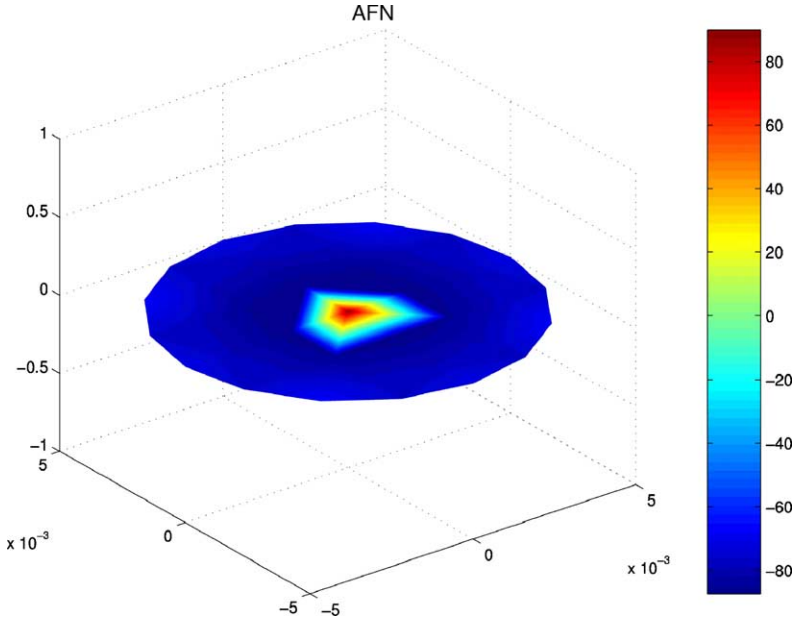

Fig. 5. Cross-section at the apex showing the value of the angle calculated using AFN method [13].

Table 2
Comparison of AFN to the Dueck method at the apex[a,b]

$\mu = 0.09$		$\mu = 0.15$		$\mu = 0.2$	
AFN	Dueck	AFN	Dueck	AFN	Dueck
90	0	90	0	90	0
−87.8287	−89.9999	−86.4223	−89.9999	−85.5935	−89.8999
−85.5519	−89.9986	−83.7236	−89.9985	−82.7164	−88.9985
−80.1776	−89.9999	−77.7033	−89.9985	−76.4056	−89.9999
−78.4363	−89.9973	−75.8757	−89.9974	−74.5503	−89.9974

[a] The other runs not presented did not differ excessively.
[b] μ has units of Pa s and density is held constant.

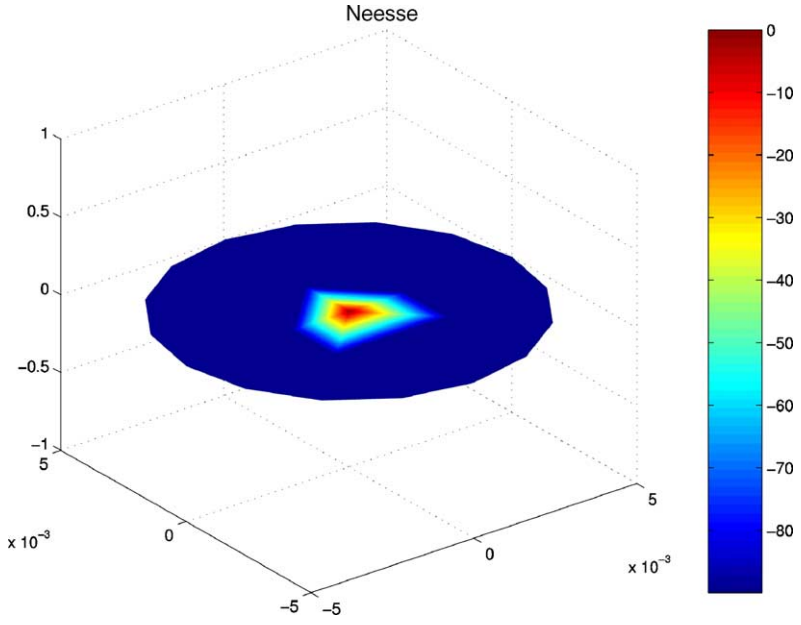

Fig. 6. Cross-section at the apex showing the value of the angle calculated using the Dueck method [7].

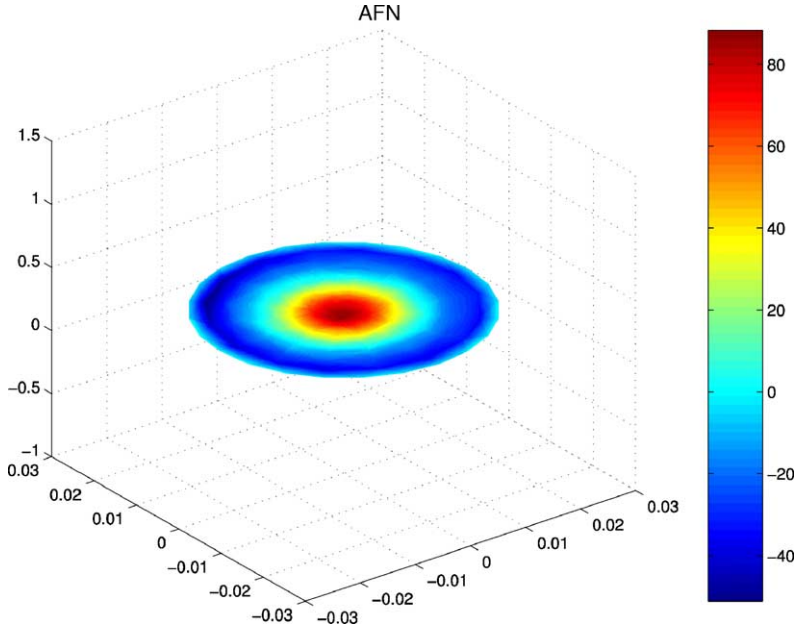

Fig. 7. Cross-section near the vortex finder showing the value of the angle calculated using AFN method [13].

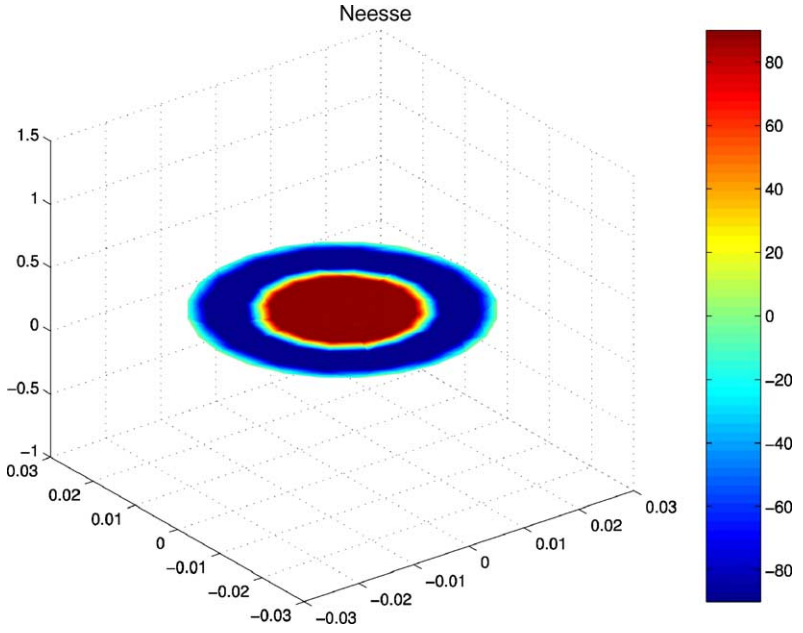

Fig. 8. Cross-section at the apex showing the value of the angle calculated using the Dueck method [11].

A comparison was made between the two different methods at the apex and right below the vortex finder exit, due to the complicated nature of the boundaries. The angles were calculated using both methods at the different cross-sections throughout the hydrocyclone. The following figures show two cross-sections at the apex using the AFN and Dueck methods.

The visual similarity between Figs. 5 and 6 are remarkable. Though at close examination of the legend, the figures illustrate that the gradient of the Dueck angle is steeper than the gradient of the AFN. However, our model predicts that at the center of the apex the actual discharge is in the upward direction, while Dueck's model does not take into account the other velocity vectors beside the tangential direction, w, and axial directions, z. The Dueck method does not predict an angle of discharge at the center of the apex, since the tangential velocity at the center is always zero for the case of axisymmetrical flow. A comparison at the top of the hydrocyclone provides additional insight into both methods.

Again, Figs. 7 and 8 show that the same basic trend of the flow is present. As shown previously, the gradient on the angle is more drastic in the Dueck model than the AFN model. An interesting occurrence happens in both cross-sections at the wall boundary. Both methods illustrate that the stresses from the boundary wall influence the angle. The predicted results qualitatively compared with the experimental results of Fisher and Flack [20], who showed that the shear stresses at the wall caused the velocity to approach or drop below zero.

4. Conclusion and future work

In conclusion, the study done on the prediction of the angle showed that both approaches tended to show similar angle profiles. Even with the simplification of the equations from three- to two-dimensional, the Dueck method shows a comparable trend to the AFN method. The differences between the two methods is the small variations in the angle calculated with increasing viscosity, which may be due to the increased pressure at the high viscosity. Additionally, experimental verification will need to be done in order to confirm whether or not one method is more accurate than the other, though the Dueck method has already been shown to work for controlling an operational cyclone. However, the trend of both methods at the wall boundary condition coincides with experimental results from Fisher and Flack [20] makes the results look very promising for both methods. The advantage of using the proposed approach is that the velocity profile and split ratio is not explicitly specified initially, thereby allowing the flow field to develop naturally. In the future, the plan is to look at assuming the presence of a non-Newtonian fluid, which allows the viscosity to change through the system. The ultimate goal of the study is to use the analysis of the discharge angle as a tool to assist in hydrocyclone design.

References

[1] K. Heiskanen, Experimental hydrocyclone roping models, Chem. Eng. J. 80 (2000) 289–293.
[2] L. Plitt, A mathematical model of the hydrocyclone classifier, Miner. Process. (CIM Bull.) (1976) 114–123.
[3] A. Lynch, T. Rao, Studies on the operating characteristics of hydrocyclone classifiers, Indian J. Technol. 6 (1968) 106–114.
[4] Nageswararao, K., Wiseman, D., Napier-Nunn, T., 2003. Two empirical hydrocyclone models revisited. In: Hydrocyclones 2003 in Capetown, South Africa.
[5] L. Chu, Q. Luo, Hydrocyclone with high sharpness of separation, Filtr. Sep. 31 (1994) 733–736.

[6] F. Concha, A. Barrientos, J. Montero, R. Sampaio, Air core and roping in hydrocyclones, Int. J. Miner. Process. 44–45 (1996) 743–749.
[7] T. Neesse, M. Schneider, J. Dueck, V. Golyk, S. Buntenbach, H. Tiefel, Hydrocyclone operation at the transition point rope/spray discharge, Miner. Eng. 17 (5) (2004) 733–737.
[8] Van Latum, L., 1992. Computed tomographic imaging of a dense media cyclone. In: Applied Research in the Minerals Industry (JKMRC).
[9] R. Williams, Measurement and modelling of slurry mixing using resistance tomography, in: Proceedings of the XIX International Mineral Processing Congress, Comminution and Simulation and Control, Society for Mining, Metallurgy, and Exploration, Inc. (AIME), 1995.
[10] K. Petersen, C. Aldrich, J. Van Deventer, C. McInnes, W. Stange, Hydrocyclone underflow monitoring using image processing methods, Miner. Eng. 9 (3) (1996) 301–315.
[11] T. Neesse, M. Schneider, V. Golyk, H. Tiefel, Measuring the operating state of a hydrocyclone, Miner. Eng. 17 (5) (2004) 697–703.
[12] J. Van Deventer, D. Feng, K. Petersen, C. Aldrich, Modelling of hydrocyclone performance based on spray profile analysis, Int. J. Miner. Process. 70 (2003) 183–203.
[13] A. Nowakowski, T. Dyakowski, Investigation of swirling flow structure in hydrocyclones, Trans. IChem.E, Part A, Chem. Eng., Res. Des. 81 (A4) (2003) 862–873.
[14] P. Gresho, Incompressible fluid dynamics: some fundamental issues, Annu. Rev. Fluid Mech. 23 (1991) 413–453.
[15] Nowakowski, A., Kraipech, W., Dyakowski, T., 2003. Analysis and Simulation of Multifield Problems. Springer, Ch. Performance of some finite elements in numerical simulation of complex incompressible three dimensional flow.
[16] P. Gresho, R. Sani, Incompressible Flow and the Finite Element Method, Wiley, 1998.
[17] V. Haroutunian, M. Engelman, I. Hasbani, Segregated finite element algorithms for the numerical solution of large-scale incompressible flow problems, Int. J. Numer. Methods Fluids 17 (1993) 323–348.
[18] P. He, M. Salcudean, I. Gartshore, A numerical simulation of hydrocyclones, Trans. IChemE 77 (1999) 429–441.
[19] L. Ma, D. Ingham, X. Wen, A numerical technique for dealing with the axis in simulating the fluid flows in polar cylindrical coordinates, Numer. Methods Laminar Turbulent Flows 10 (1997) 203–214.
[20] M. Fisher, R. Flack, Velocity distributions in a hydrocyclone separator, Exp. Fluids 32 (2002) 302–312.